Reconstruction of Brain Tissue Surface Based on Three-Dimensional T1-Weighted MRI Images

Wenchao Lv*, Yahui Peng*, Chao Yang†and Xinchun Li‡
*School of Electronic and Information Engineering
Beijing Jiaotong Unversity, Beijing, China
Tel: +861051683680 Fax: +861051683682
†The Department of Neurosurgery
The First Affiliated Hospital, Sun Yat-sen University, Guangzhou, China
‡The Department of Radiology
The First Affiliated Hospital of Guangzhou Medical School, Guangzhou, China

***Abstract*—Three-dimensional (3D) T1-weighted magnetic resonance imaging (MRI) is an important technique for accurate localization and evaluation of brain tumors. A fast-forming technique was proposed in this study based on 3D MRI and 3D printing to generate a physical 3D model that might help improve the neurosurgery planning for brain tumors. In this paper, a brain tissue segmentation and reconstruction method is presented using the unified segmentation algorithm and 3D interpolation. Results showed that the quality of the 3D brain tissue reconstruction was acceptable and linear interpolation of the 3D model improved the visualization of the brain surface morphology. We conclude that image segmentation and reconstruction of brain tissue based on the 3D T1-weighted MRI is feasible for fast 3D prototyping and it may help neurosurgeons for the surgery planning.**

***Keywords-component*—magnetic resonance imaging, 3-dimensional T1-weighted imaging, brain tissue, surface reconstruction, segmentation**

I. Introduction

Brain tumor is one of the major threats to human health. In the USA, more than 22,000 people are diagnosed with brain tumors every year [1]. Brain surgery is a treatment commonly used for a number of brain diseases such as glioma, arteriorvenous malformation, and epilepsy. However, the risk of the brain surgery is high and the prognosis is difficult to predict [2], [3]. To reduce the potential risk of the brain surgery, it is necessary to make a detailed plan before the surgery, and imaging techniques are often used for this purpose. Due to its excellent soft tissue contrast and high spatial resolution, 3D T1-weighted MRI is a widely used imaging technique for the surgery planning. Based on the 3D T1-weighted MRI, brain tissue, skulls, and other tissues can be reconstructed virtually and displayed on a computer screen. Neurosurgeons could manipulate the virtually constructed brain to mimic what would happen during the surgery. However, the 3D model on the screen is still "virtual", meaning neurosurgeons can only perceive the spatial information from a 2D projection of the 3D model. This significantly restricts the utilities of the virtual 3D model on the computer screen. One step forward, we are proposing to develop a fast forming technique based on 3D MRI and 3D printing to generate a physical 3D model including brain tissue, skull, and other surrounding tissues. Using the physical 3D model, neurosurgeons are free to perform all possible surgical procedures for a better surgery planning.

In this preliminary study, we investigate brain tissue segmentation techniques and study the feasibility of making 3D brain models using a general-purposed 3D printer, and the 3D brain model is composed of binary 2D image sets. The main aspects of this study are the segmentation of brain and other head tissues, smoothing of the segmented brain tissue, and image format conversion for 3D printing. In the end, we obtain a 3D binary model as the result of the processing of gray level magnetic resonance (MR) images.

The remainder of this paper is organized as follows. The characteristics of patients and relevant MR imaging protocols are given in Section 2.1. The 3D brain tissue segmentation and reconstruction methods are described in Section 2.2. The experimental results are presented in Section 3. Section 4 discusses the bias-field effect and the future work. Finally, we conclude the paper in Section 5.

This study was supported in part by Beijing Jiaotong University Fund W15JB00470 and Science Technology Project of Beijing D151100000415002.

II. Materials and Methods

A. Patients

This study was approved by the institutional review board at each of the participating medical institutions. We collected four 3D T1-weighted MR images for the experiment. Sensitive patient health information was properly anonymized. The characteristics of the patients are shown in Table 1.

TABLE I
THE CHARACTERISTICS OF THE PATIENTS

	Age (year)	Gender	MR Scanner	Weight (kg)
Case1	47	Male	PHILIPS	60
Case2	47	Male	PHILIPS	80
Case3	88	Male	PHILIPS	50
Case4	73	Male	PHILIPS	70

978-1-4673-9098-9/15/$31.00 ©2015 IEEE

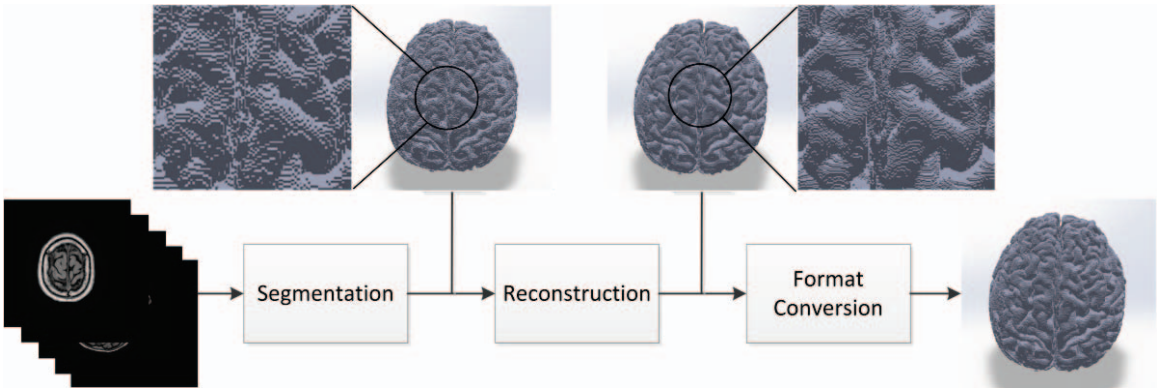

Fig. 1. Flowchart of the methods used in this study. Three steps are included: segmentation, reconstruction, and format conversion.

TABLE II
THE CHARACTERISTICS OF THE PATIENTS

	Repetition Time (ms)	Echo Time (ms)	Slice Thickness (mm)	Field Strength (Tesla)	Pixel Spacing (mm)
Case1	25.00	3.84	2.00	1.5	[0.51,0.51]
Case2	25.00	3.82	2.00	1.5	[0.51,0.51]
Case3	25.00	1.94	2.00	3.0	[0.87,0.87]
Case4	25.00	1.97	2.00	3.0	[0.87,0.87]

B. MR Imaging

Two types of MR machines were used for image acquisition: a 1.5-Tesla Philips (Archieva, Philips Healthcare, Eindhoven, the Netherlands) with a SENSE-NV-16 head coil and a 3.0-Tesla Philips (Archieva3.0, Philips Healthcare, Eindhoven, the Netherlands) with a SENSE-Head-8 coil. For the 3D T1-weighted imaging, the detailed imaging parameters are listed in Table 2.

C. Methods

As shown in Fig. 1, three steps are included in this study: brain tissue segmentation, 3D image reconstruction, and image format conversion. In the first step, the unified segmentation (US) method was employed to segment the brain tissue [4]. To ensure high spatial resolution for 3D printing, an interpolation method was used in the second step. Finally, the model data was converted to the industry standard format for 3D printing.

1) Brain tissue Segmentation: We used the US method for brain tissue segmentation. The basic idea of the method relied on an atlas of the human brain, which introduced *a priori* based on a previous collected database. At first, the brain MR image to be segmented was registered to the atlas, then a Gaussian mixture model (GMM) was used to segment different tissue components according to the gray levels of registered voxels. Because the bias field in the MR images could substantially influence the segmentation results, the bias field should be corrected before the registration and segmentation. In the US method, the bias-field correction, image registration, and image segmentation were finished in a single iterative procedure [4].

Bias field is caused by the uneven sensitivity of the coil elements [5]–[8]. Correction of the bias field is a challenging task in MRI image processing. Depending on the relationship of MRI signal and noise, a number of different models were proposed [6]. In this study, a log-space model was employed to represent the bias field, which is defined as,

$$y_i = \mu_i e^{n_i} / \rho_i \tag{1}$$

where y_i is the measured signal at pixel i, μ_i is the actual signal of pixel i without bias, n_i is the noise signal, and ρ_i is the effect of the bias field, which is assumed to follow a Gaussian distribution.

The grey-level distribution was modeled by a mixture of *K* Gaussian distributions. Based on the combination of the field model and Gaussian mixture model, the probability of the entire dataset was defined as,

$$P(y|\beta,\alpha,\gamma,\mu,\sigma^2) = \prod_{i=1}^{I}(\sum_{k=1}^{K} \frac{\gamma_k b_{ik}(\alpha)}{\sum_{k=1}^{K}\gamma_k b_{ik}(\alpha)} \frac{\rho_i(\beta)}{(2\pi\sigma_k^2)^{\frac{1}{2}}} \exp(-\frac{(\rho_i(\beta)y_i - \mu_k)^2}{2\sigma_k^2})) \tag{2}$$

where y is the entire dataset of pixels, β is the vector of bias field effect, α is the vector stands for the effect of the brain tissue probability atlas, γ_k is the vector of mixing proportion for class k, μ_k and δ_k are the Gaussian mixture distribution parameters of class k, b_{ik} is the prior probability for class k of pixel i. In order to segment the images, the Gaussian mixture distribution parameters were determined when the probability of the entire dataset was maximized. We then defined a cost

function as,

$$\varepsilon = -\sum_{i=1}^{I} \log\left(\frac{\rho_i(\beta)}{\sum_{k=1}^{K} \gamma_k b_{ik}(\alpha)} \sum_{k=1}^{K} \frac{\gamma_k b_{ik}(\alpha)}{(2\pi\sigma_k^2)^{\frac{1}{2}}} \exp\left(-\frac{(\rho_i(\beta) y_i - \mu_k)^2}{2\sigma_k^2}\right)\right) \quad (3)$$

When ϵ was minimized, the most probable parameters of the Gaussian mixture distribution parameters could be calculated. As the brain shape was estimated by the brain tissue probability atlas, the conditional probability of the entire dataset was defined as,

$$P(y, \beta, \alpha | \gamma, \mu, \sigma^2) = P(y|\beta, \alpha, \gamma, \mu, \sigma^2) P(\beta) P(\alpha) \quad (4)$$

We then defined another cost function,

$$f = -\log P(y, \beta, \alpha | \gamma, \mu, \sigma^2) = \varepsilon - \log P(\beta) - \log P(\alpha) \quad (5)$$

When this cost function was minimized, the most probable Gaussian mixture model parameters μ and δ were determined. Subsequently, pixels were classified by the Gaussian mixture model.

Five tissue components were extracted from the 3D T1-weighted MR images: gray matter, white matter, cerebrospinal fluid, skull, and other structures. Because neurosurgeons are mostly concerned with the morphology of the brain tissue, gray matter and white matter were merged together as one structure, which is referred as "brain tissue" in this study.

2) 3D Reconstruction: Because the original 3D T1-weighted MR image was anisotropic, the resolution in the head-to-toe direction was lower than that of the other two directions. Due to this anisotropy, 3D reconstruction of the brain tissue often had a strong stair artifact, especially along the head-to-toe direction. To eliminate the artifact and improve the visualization, we applied the trilinear method to interpolate the segmentation result into a higher resolution and to make the image isotropic [9], [10].

Trilinear interpolation is a method of multivariate interpolation in a 3D space. It approximates the value of a point (V_p) at arbitrary location by its eight neighborhood pixels with different weights (Fig. 2). The grey level of the interpolated point is defined as,

$$V_p = \frac{\sum_{j=0}^{7} V_{7-j} \left|(x_j - x)(y_j - y)(z_j - z)\right|}{(x_7 - x_0)(y_7 - y_0)(z_7 - z_0)} \quad (6)$$

where V_p is the grey level of the interpolated point (x, y, z) in the cube, specified by the eight neighborhood pixels of V_p. V_{7-j} is the point diagonally opposite of V_i, the denominator in (6) is to normalize the V_p. The weight of a neighborhood point is measured by the product of distance. The farther the distance is, the lighter the weight is.

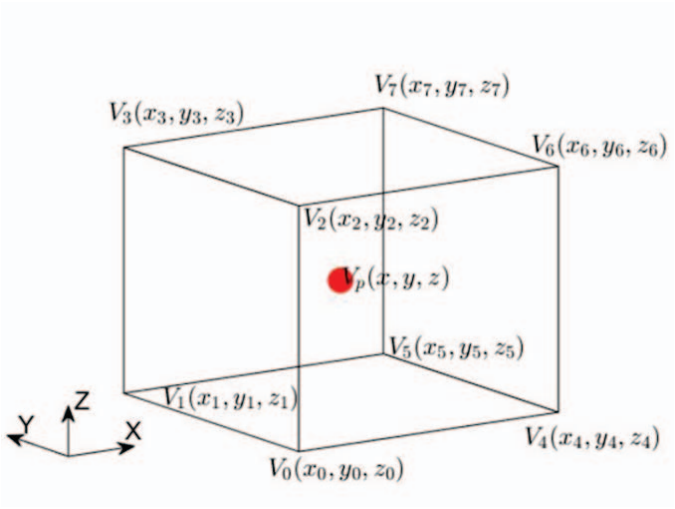

Fig. 2. Diagram of Trilinear.V_p is the point to be interpolated. V_j,j=0-7 are the original points near V_p.

3) Format Conversion: To ensure that the isometric 3D brain tissue could be accepted by a 3D printer, we converted the interpolated segmentation results to the industry standard for 3D printing, the STereoLithography (STL) format, a widely accepted protocol in computer-aided manufacturing [11]. Original triangulated surface are describe in this format without any representation of color, texture or other common attributes.

III. Result

Both 1.5-Tesla and 3.0-Tesla MR images were segmented in this study. Although the morphology of the brains is diverse, reasonable segmentation results are obtained. An overhead view of the brain tissue is chosen to show the texture, by which we can see most of the gyri. As show in Fig. 3, the brain surface texture of the 3.0-Tesla MR images is more subtle and finer than that of the 1.5-Tesla images. In order to improve visual perception, 3D rendering graphics was employed to generate Fig. 3. The morphology of the gyri looked natural, which is helpful for neurosurgeons to orientate and locate the brain tumor accurately. In Fig. 3, the gyri in (c) and (d) are more obvious than gyri in (a) and (b). The final reconstruction results were in STL format. Comparing with the segmentation results in Fig. 4, the stair artifact was reduced in the interpolated images, and therefore, the brain surface was smoother. The shadow in Fig. 4 is caused by the illumination of the light sources in the 3D rendering.

IV. Discussion

In recent years, a number of methods have been proposed for brain tissue segmentation. These methods can be roughly classified into two classes: (a) atlas-based approach, which relies on *a priori* knowledge for atlas generation [5], [12]; (b) clustering-based approaches, which may be implemented by the use of the mean shift method [13]. Other approaches also used methods such as GMM-based technique [4]. In this study, we adopted the US method [4]. The US is a method

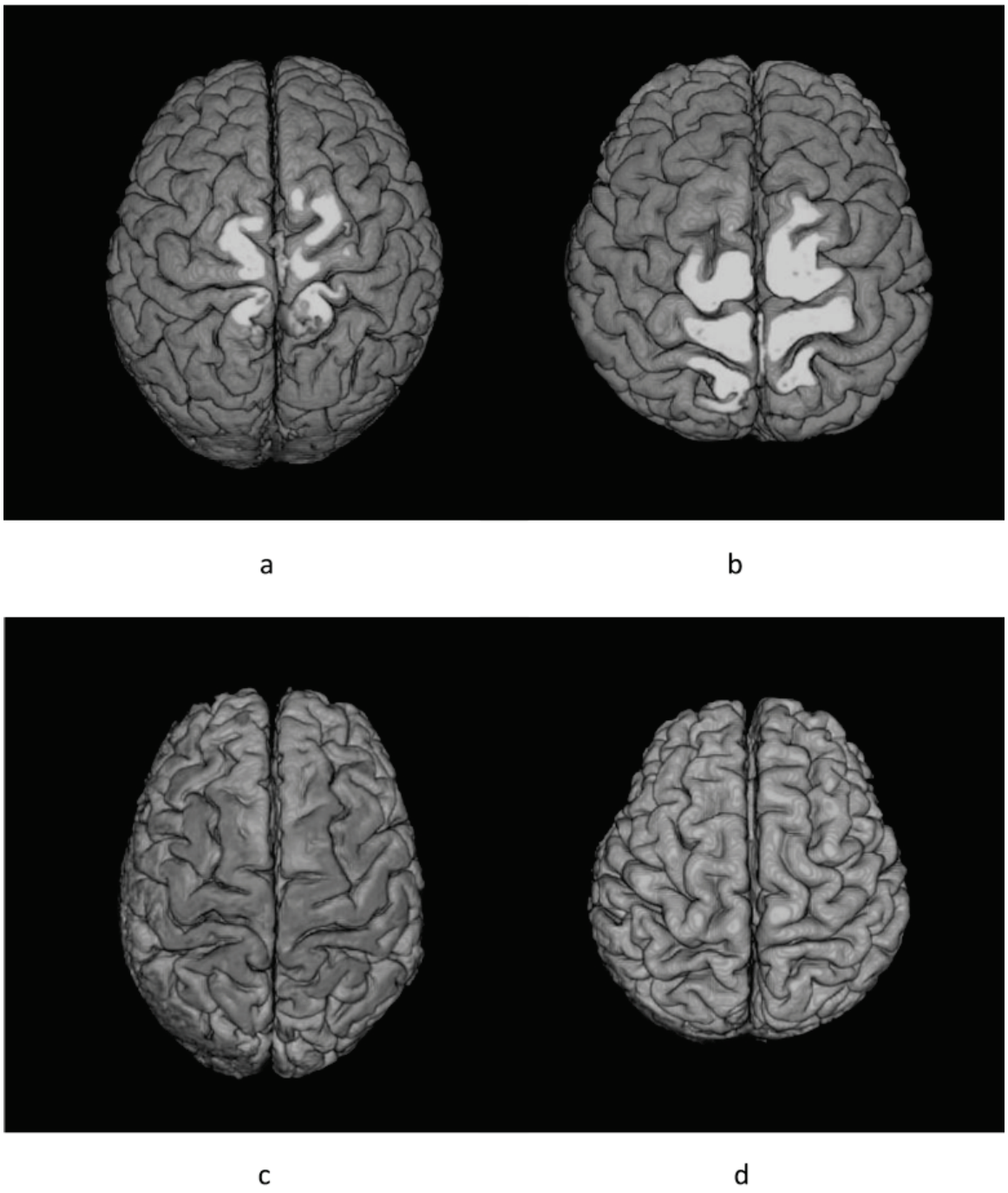

Fig. 3. Results of brain tissue reconstruction. Segmentation results of 1.5-Tesla images (top) and segmentation results of 3.0-Tesla images (bottom) are displayed. Note that the brain tissue is truncated for the 1.5-Tesla images during MR image acquisition. Visual evaluation indicates that the morphology of the gyri in results (c) and (d) are slightly better than that in results (a) and (b).

that combines the bias-field correction, image registration, and image segmentation in a single iterative procedure which is appropriate to our requirement. Bias field correction is a necessary step for accurate segmentation [14]. In this study, images in different field strength were used, and the bias field phenomenon might not be the same. According to the segmentation results, the influence of the bias field was observed in the occipital lobes for both 3.0-Tesla images and 1.5-Tesla images. Except that, the influence of the bias field was minimal in the four cases. Preprocessing such as image enhancement may increase the accuracy of segmentation and correct the bias field. Trilinear interpolation is considered a straightforward and practical method. Visually, the 3D rendering of the segmented results were improved by the trilinear interpolation, which might help improve the fidelity of 3D printing. As the accuracy of the 3D model is an important

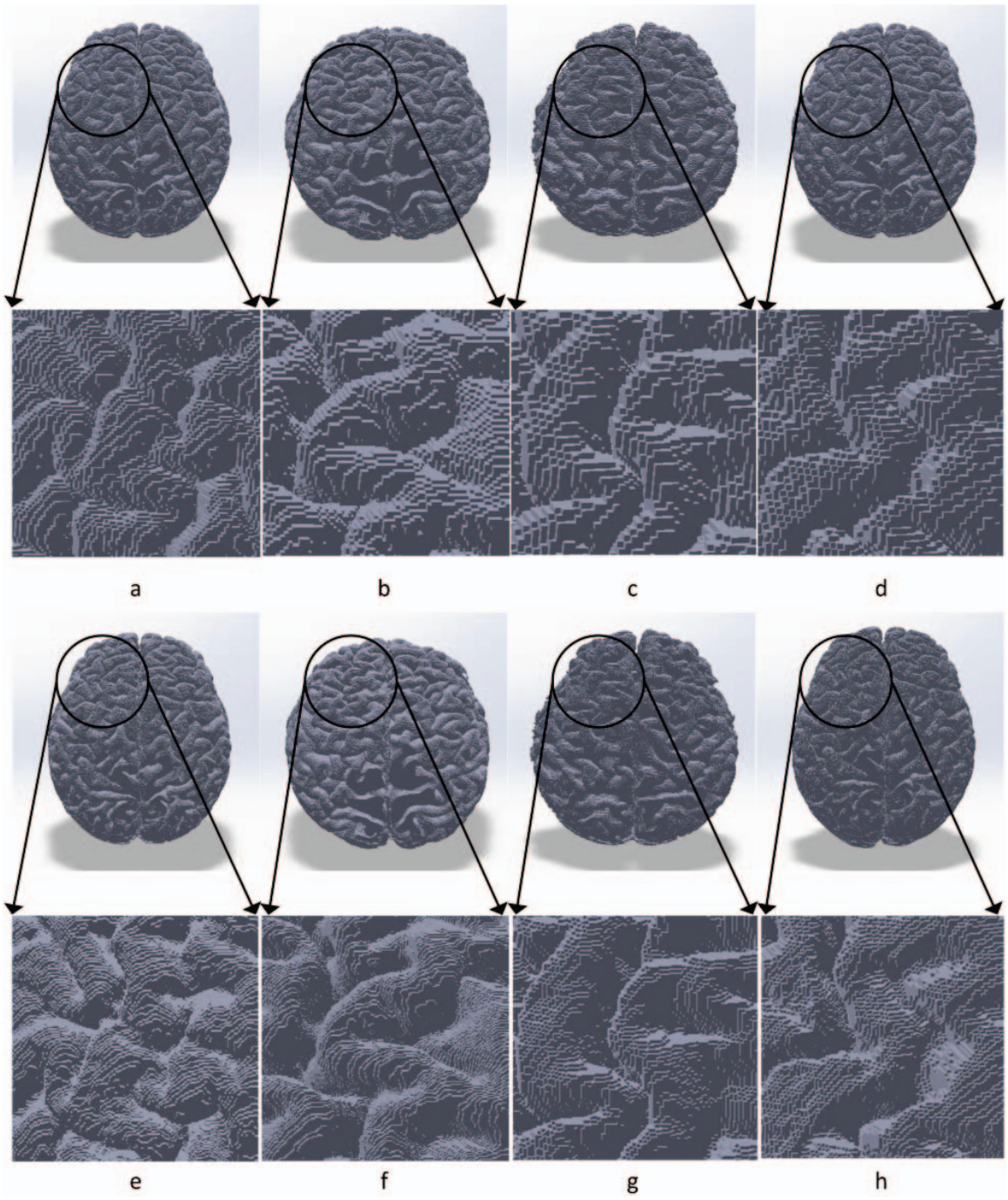

Fig. 4. Results of reconstruction in stereolithography (STL) format. From top to bottom: segmentation results, details of the segmentation, interpolation result, and details of the interpolation. The columns from left to right correspond to case1-4, respectively.

factor to improve the cognitive ability of neurosurgeons to perform neurosurgical planning. The reconstruction of brain tissue surface has achieved in theory. 3D printing is a new technology for rapid prototyping manufacturing. But, since the technical parameters (such as size of this workspace, accuracy, material) of a 3D printer are uncertain, the 3D printer is still in selection. We will accomplish the brain tissue printing and provide some result comparison with existing methods in our future study.

V. Conclusion

In this study, a 3D image reconstruction method based on US segmentation and trilinear interpolation is implemented for brain tissue reconstruction. We conclude that image segmentation and reconstruction of brain tissue based on the 3D T1-weighted MRI is feasible for fast 3D prototyping, which

we can improve cognitive ability of neurosurgeon to perform neurosurgical planning.

ACKNOWLEDGMENT

The authors would also like to thank P. Li, F. Li and Y. Ma for assisting in sorting data, and the anonymous reviewers for their valuable comments.

REFERENCES

[1] J. F. Hainfeld, H. M. Smilowitz, M. J. O'Connor, F. A. Dilmanian, and D. N. Slatkin, "Gold nanoparticle imaging and radiotherapy of brain tumors in mice," *Nanomedicine*, vol. 8, no. 10, pp. 1601–1609, 2013.

[2] S. V. Bhujbal, P. de Vos, and S. P. Niclou, "Drug and cell encapsulation: alternative delivery options for the treatment of malignant brain tumors," *Advanced drug delivery reviews*, vol. 67, pp. 142–153, 2014.

[3] J. Böttger, D. S. Margulies, P. Horn, U. W. Thomale, I. Podlipsky, I. Shapira-Lichter, S. J. Chaudhry, C. Szkudlarek, K. Mueller, G. Lohmann *et al.*, "A software tool for interactive exploration of intrinsic functional connectivity opens new perspectives for brain surgery," *Acta neurochirurgica*, vol. 153, no. 8, pp. 1561–1572, 2011.

[4] J. Ashburner and K. J. Friston, "Unified segmentation," *Neuroimage*, vol. 26, no. 3, pp. 839–851, 2005.

[5] C. Li, R. Huang, Z. Ding, J. C. Gatenby, D. N. Metaxas, and J. C. Gore, "A level set method for image segmentation in the presence of intensity inhomogeneities with application to mri," *Image Processing, IEEE Transactions on*, vol. 20, no. 7, pp. 2007–2016, 2011.

[6] U. Vovk, F. Pernuš, and B. Likar, "A review of methods for correction of intensity inhomogeneity in mri," *Medical Imaging, IEEE Transactions on*, vol. 26, no. 3, pp. 405–421, 2007.

[7] J. G. Sled, A. P. Zijdenbos, and A. C. Evans, "A nonparametric method for automatic correction of intensity nonuniformity in mri data," *Medical Imaging, IEEE Transactions on*, vol. 17, no. 1, pp. 87–97, 1998.

[8] P.-L. Bazin and D. L. Pham, "Topology correction of segmented medical images using a fast marching algorithm," *Computer methods and programs in biomedicine*, vol. 88, no. 2, pp. 182–190, 2007.

[9] B. Zhuge, H.-q. Feng, and H.-q. Zhou, "A fast tri-linear interpolation algorithm for volume rendering of medical images," *SPACE MEDICINE AND MEDICAL ENGINEERING*, vol. 16, no. 3, pp. 206–209, 2003.

[10] D. Rajon and W. Bolch, "Marching cube algorithm: review and trilinear interpolation adaptation for image-based dosimetric models," *Computerized Medical Imaging and Graphics*, vol. 27, no. 5, pp. 411–435, 2003.

[11] G. G. Jacob, C. C. Kai, and T. Mei, "Development of a new rapid prototyping interface," *Computers in Industry*, vol. 39, no. 1, pp. 61–70, 1999.

[12] L. Wang, F. Shi, G. Li, Y. Gao, W. Lin, J. H. Gilmore, and D. Shen, "Segmentation of neonatal brain mr images using patch-driven level sets," *NeuroImage*, vol. 84, pp. 141–158, 2014.

[13] L. Lin, D. Garcia-Lorenzo, C. Li, T. Jiang, and C. Barillot, "Adaptive pixon represented segmentation (aprs) for 3d mr brain images based on mean shift and markov random fields," *Pattern Recognition Letters*, vol. 32, no. 7, pp. 1036–1043, 2011.

[14] K. Kim, P. Habas, V. Rajagopalan, J. Scott, J. M. Corbett-Detig, F. Rousseau, O. Glenn, C. Studholme *et al.*, "Bias field inconsistency correction of motion-scattered multislice mri for improved 3d image reconstruction," *Medical Imaging, IEEE Transactions on*, vol. 30, no. 9, pp. 1704–1712, 2011.